Published in final edited form as:
J Proteome Res. 2010 April 5; 9(4): 1786–1794. doi:10.1021/pr900909t.

Vimentin Is a Functional Partner of Hormone Sensitive Lipase And Facilitates Lipolysis

Wen-Jun Shen[1], **Shailja Patel**[1], **John E. Eriksson**[2], and **Fredric B. Kraemer**[1,*]

[1] Division of Endocrinology, Stanford University and VA Palo Alto Health Care System, Palo Alto, CA 94304 [2] Department of Biology, Åbo Akademi University, Turku, Finland

Abstract

Lipolysis involves a number of components including signaling pathways, droplet-associated proteins and lipases such as hormone-sensitive lipase (HSL). We used Surface Enhanced Laser Desorption/Ionization time-of-flight mass spectroscopy to identify cellular proteins that might interact with HSL and potentially influence lipolysis. Using recombinant HSL as bait on protein chips, clusters of proteins of 14.7 to 18.9 kDa, 25.8–26.8 kDa, 36.1 kDa, 44.3–49.1 kDa, and one at 53.7 kDa were identified that interact with HSL, particularly when lysates were examined from β-agonist treated mouse adipocytes. The ability to detect these interacting proteins was markedly diminished when the adipocytes were treated with insulin. A very similar pattern of proteins was identified when anti-HSL IgG was used as the bait. Following immunocapture, the identification of the prominent 53.7 kDa protein was carried out by tryptic digestion and MS analysis, and determined to be vimentin. The interaction of HSL with vimentin, and its hormonal dependence, was confirmed by co-immunoprecipitation. β-agonist stimulated lipolysis and the rate of HSL translocation were impaired in vimentin null adipocytes, even though normal amounts of lipases and droplet-associated proteins are expressed. The current studies provide evidence that vimentin participates in lipolysis through direct, hormonally regulated interactions with HSL.

Keywords

adipose; surface enhanced laser desorption/ionization time-of-flight mass spectroscopy; translocation

Introduction

Adipose tissue constitutes the major repository of energy stores for vertebrate organisms. For this stored energy to be utilized, it is necessary for the triacylglycerols (TAG) in adipose tissue to be mobilized to free fatty acids (FFA) and then released into the circulation, the process of adipocyte lipolysis. Lipolysis is principally controlled by the activity of the sympathetic nervous system and by circulating levels of insulin. Thus, catecholamines, acting through β-adrenergic receptors, stimulate lipolysis by activating adenylyl cyclase and raising intracellular concentrations of cyclic AMP, with resultant activation of cyclic AMP-dependent protein kinase (PKA) [1]; however, β-adrenergic receptors can also activate extracellular signal-regulated kinases (ERK1/2) that stimulate lipolysis [2, 3]. The major adipose protein targets that are phosphorylated by PKA are hormone-sensitive lipase (HSL) [4] and perilipins [5]. Perilipin is

*Corresponding author: Fredric B. Kraemer, M.D., Division of Endocrinology, S-025, Stanford University, Stanford, CA 94305-5103, Telephone: 650-493-5000 ext 63184, Fax: 650-852-3263, fbk@stanford.edu.

found on the surface of the lipid droplet along with other droplet-associated proteins, specific marker proteins, structural proteins, enzymes involved in various aspects of cholesterol and fatty acid metabolism, and proteins that function as regulators of membrane traffic [6, 7].

The chief enzyme responsible for the mobilization of FFA from adipose tissue was thought to be HSL. HSL is highly expressed in adipose tissue, and has broad substrate specificity, catalyzing the hydrolysis of TAG, diacylglycerol (DAG), monoacylglycerol (MAG), and cholesteryl esters, as well as retinyl esters; however, it possesses no phospholipase activity [4]. The hydrolytic activity of HSL against TAG and cholesteryl esters, but not against DAG, is stimulated by phosphorylation mediated primarily by PKA [4]. It had long been considered that HSL [4] was the rate limiting enzyme for lipolysis; however, examination of the HSL null mouse indicated the existence and importance of other lipases [8]. Adipose triglyceride lipase (ATGL), also known as desnutrin [9], calcium independent phospholipase $A_2\zeta$[10], and patatin-like phospholipase A2 [11], was identified in adipose tissue, shown to catalyze the initial step of TAG hydrolysis to DAG, but to lack DAG hydrolase activity [12], and to be the rate-controlling enzyme for the initiation of PKA-stimulated lipolysis in murine cells [13–15]. In contrast to HSL, ATGL does not appear to be directly regulated by PKA phosphorylation. Efficient TAG hydrolysis by ATGL requires activation by comparative gene identification-58 [16]. In combination, HSL and ATGL appear to account for >95% of TAG hydrolase activity in murine adipose cells [17].

PKA-stimulated lipolysis is paralleled by a translocation of HSL from the cytosol to the surface of the lipid droplet [18, 19]. The mechanisms mediating the translocation of HSL have not been fully elucidated, but translocation is dependent on the phosphorylation of HSL [20]. Either no or only modest movement of ATGL to the lipid droplet is observed with PKA-stimulation [12, 21]. Whereas PKA-mediated phosphorylation of perilipin is required for stimulated lipolysis, the translocation of HSL to the lipid droplet is dependent on perilipin [22], but independent of phosphorylation of perilipin [15]. The current studies used Surface Enhanced Laser Desorption/Ionization (SELDI) time-of-flight mass spectroscopy (TOF-MS) to identify cellular proteins that might interact with HSL and, in this manner, participate in regulating the function of HSL in mediating lipolysis. We provide evidence that vimentin, an intermediate filament protein, interacts with HSL in a hormonally-dependent manner and facilitates lipolysis.

Materials and Methods

Chemicals and reagents

Reagents were obtained from the following sources: Bovine serum albumin (fraction V) from Sigma, St. Louis, MO, USA; ECL western blotting detection reagents, horseradish peroxidase-linked whole antibody anti-rabbit IgG, from Amersham Life Sciences Products, Arlington Heights, IL, USA; BCA protein kits from Pierce Biotechnology, Inc., Rockford, IL, USA; nitrocellulose paper from Schleicher and Schuell, Keene, NH, USA; organic solvents were from J.T. Baker, Phillipsburg, NJ, USA; TRIzol reagent and SuperScript II from Invitrogen, Carlsbad, CA, USA; RNeasy kit from QIAGEN, Valencia, CA, USA; SyBr green Taqman PCR kit from Applied Biosystems, Foster City, CA, USA; anti-ATGL antibodies, phospho-ERK and total ERK from Cell Signaling Technology, Danvers, MA, USA; antibodies against β-actin, ADRP, and TIP47 from Santa Cruz Biotechnology, Santa Cruz, CA, USA; antibodies against vimentin from Abcam Inc., Cambridge, MA, USA; Odyssey blocking buffer, goat anti-mouse IgG-IR dye 800cw, and donkey anti-goat IgG-IR dye 680cw, goat anti-rabbit IgG-IR dye 680cw from Li-Cor Biosciences, Lincoln, NE, USA. Glycerol assay kit from Stanbio, Boerne, TX, USA. All other reagents were from Sigma, St. Louis, MO, USA, unless otherwise noted. Anti-mouse full-length HSL IgG was prepared as described previously [23]. Anti-perilipin antibody was a gift from Dr. Andrew S. Greenberg from Tufts University. Anti-CGI-58 antibody was a gift of Dr. Takashi Osumi from the University of Hyogo, Japan.

Animals and adipose cell isolation and incubations

Wild-type control C57Bl6J mice on an ad libitum diet were used for most experiments. Vimentin null mice on a 129 background were generated as previously described [24]. Mice heterozygous for the deleted vimentin allele were bred to generate vimentin−/− and vimentin +/+ wild-type littermates. Genotyping was performed as described previously [24]. Adipocytes were prepared from epididymal fat pads by collagenase digestion and floatation as described previously [25]. Adipocytes isolated from 12–16 wks old C57Bl6J mice were incubated in the absence or presence of isoproterenol (1 μM) ± insulin (100 μU/ml) in 120 mM NaCl, 4 mM KH_2PO_4, 1 mM $MgSO_4$, 1 mM $CaCl_2$, 10 mM $NaHCO_3$, 27 mM HEPES (pH 7.4) containing 3% BSA and 2.5 mM glucose for 30 min at 37°C in 95% air-5% CO_2. At the end of the incubation, cells were washed, lysed in 20 mM Tris-HCl (pH 7.4), 1 mM EDTA, and 260 mM sucrose with proteinase inhibitors, centrifuged at 16,000 *g* for 15 min, and the supernatants taken for study. For lipolysis studies, adipocytes isolated from 12–16 wks old vimentin−/− (weights 27.7±1.1 to 28.0±1.1 gm) and wild-type (weights 27.5±1.6 to 29.8±1.7 gm) littermates were incubated in the absence or presence of isoproterenol (various concentrations) in 120 mM NaCl, 4 mM KH_2PO_4, 1 mM $MgSO_4$, 1 mM $CaCl_2$, 10 mM $NaHCO_3$, 27 mM HEPES (pH 7.4) containing 3% BSA and 2.5 mM glucose for 60 min at 37°C in 95% air-5% CO_2. At the end of the incubation, an aliquot of infranatant was removed for measurement of glycerol concentration. For translocation studies, adipocytes isolated from vimentin−/− and wild-type littermates were incubated with isoproterenol (1 μM) as above for various times at 37°C in 95% air-5% CO_2. At the indicated times the cells were washed, homogenized, the fat cake and cytosol separated by centrifugation, and HSL detected by immunoblotting as described previously [19, 26] and below. Adipose cell size was determined by measuring the diameter of 100 adipose cells per animal by microscopy of paraformaldehide fixed epididymal adipose tissue [27].

Immunoblotting and immunoprecipitation

Immunoblotting was performed as described previously [26]. Briefly, adipose cells were homogenized in 50 mM Tris-HCl, pH 7.4, 8% sucrose, 1 mM EDTA, 0.1 mM Na_3VO_4, 50 mM NaF, with 10 μg/ml leupeptin and protein concentrations were determined by BCA protein assays. Approximately 20 μg proteins were resolved by 4–15% gradient SDS-PAGE gel and blotted onto nitrocellulose membranes. Membranes were blocked with Odyssey blocking buffer for 2h at room temperature and were incubated with primary antibodies at the following dilutions: anti-ATGL (1:1000), anti-HSL (1:5000), anti-CGI-58 (1:1000), anti-Plin (1:1000), anti-ADRP (1:1000), anti-TIP47 (1:1000), anti-β-actin (1:1000), anti-phospho-ERK (1:1000), anti-total ERK (1:1000). Membranes were incubated with the appropriate secondary antibody conjugated to infra red dye (goat anti-mouse IgG-IR dye 800cw, and donkey anti-goat IgG-IR dye 680cw, goat anti-rabbit IgG-IR dye 680cw) at room temperature for 1h, washed 3 times with PBS (0.1% Tween 20), rinsed with PBS, then detected by an Odyssey Infrared Fluorescent Imaging System (Li-Cor Biosciences, Lincoln, NE). Alternatively, membranes were incubated with anti-phospho-ERK (1:1000), anti-total ERK (1:1000) or anti HSL (1:5000) and then with horseradish peroxidase-linked anti-rabbit IgG. The membranes were visualized with chemiluminescence reagent ECL, exposed to Kodak XAR film, and then analyzed by a Fluor-S multi-image analyzer (Bio-Rad, Hercules, CA). Immunoprecipitation was performed as described previously [28]. Briefly, adipose cells were homogenized in 50 mM Tris-HCl, pH 7.4, 8% sucrose, 1 mM EDTA, 0.1 mM Na_3VO_4, 50 mM NaF, with 10 mg/ml leupeptin and protein concentrations were determined by BCA protein assays. An aliquot (250 μg) was precleared with Protein A beads and then incubated with an immunomatrix consisting of rabbit polyclonal anti-HSL IgG and protein A. After overnight incubation at 4°C, the immune complex was centrifuged at 10,000 × *g* for 15 min and washed twice in PBS with 0.05% BSA and then twice in PBS. The pellet was resuspended in SDS-PAGE loading buffer (0.063 M Tris-HSL pH 6.8, with 1% 2-mercaptoethanol, 1% SDS, and 13% (v/v) glycerol), boiled for 5 min,

electrophoresed on 12% SDS-PAGE, transferred to nitrocellulose paper, and immunoblotted with anti-vimentin IgG (1:2000).

PCR analysis

Adipose tissue was homogenized in TRIzol reagent and total RNA was extracted and purified using the RNeasy kit, and treated with RNase-free DNase I. Total RNA was reverse-transcribed in a 20μl reaction containing random primers and Superscript II enzyme. Real-time PCR was performed with an ABI Prism 7900 System using SYBR green master mix reagent and specific primer pairs as described previously [26, 29]. The relative mass of specific RNA was calculated by the comparative cycle of threshold detection method according to the manufacturer's instruction. Three independent sets of Taqman real time PCR were performed using different RNA preparations from adipose tissue; each run of Taqman real-time PCR was conducted in triplicate.

Recombinant HSL

Recombinant His_6-HSL was produced from S*f*21 cells and purified by Ni-agarose chromatography as described previously [30]. Recombinant His-HSL (0.2 mg/ml) was stored in 50 mM $NaPO_4$, 300 mM NaCL, 200 mM imidizole (pH 6), and 10% glycerol until use, when it was dialyzed 2 times against 1 L phosphate buffered saline.

Protein-Protein interactions using SELDI-TOF-MS

Proteins were immobilized on ProteinChip® Arrays (Ciphergen Biosystems, Fremont, CA, USA, now BioRad Laboratories) through incubation for 2 h at room temperature in a humidified chamber. Initial experiments tested 3 different arrays, PS10, PS20 and RS100. PS10 and RS100 are preactivated with carbonyldiimidazole functional groups, whereas PS20 is preactivated with epoxide chemistry. RS100 yielded cleaner background and capacity when recombinant HSL was used as bait, whereas PS10 yielded cleaner background when anti-HSL IgG was used as bait. Consequently, recombinant HSL (2 μl, ~0.5 μg) or BSA was immobilized on RS100 arrays and anti-HSL IgG (4μg) or BSA was immobilized on PS10 arrays and used for studies. Unreacted amine groups were blocked with 0.5 M ethanolamine/phosphate-buffered saline for 1 h. The ProteinChips were washed three times for 5 min with phosphate-buffered saline containing 0.1% Triton X-100. Freshly prepared adipocyte lysates (2–4 mg/ml) were incubated with the arrays, then washed twice for 5 min with phosphate-buffered saline containing 0.1% Triton X-100 and once for 3 min with Tris-HCl buffer (pH 9.0) containing 1 M urea, 2% CHAPS, and 0.5 M NaCl. The ProteinChips were rinsed with 5 mM HEPES (pH 7.2) for 15 s and air-dried. A saturated solution of 3,5-dimethoxy-4-hydroxyinnamic acid (sinapinic acid) in 50% acetonitrile and 0.5% trifluoroacetic acid was applied to the ProteinChips and mass analysis was performed by SELDI-TOF-MS using the ProteinChip Biology System II and Ciphergen software version 3.0 (Ciphergen Biosystems, Fremont, CA, USA). Spectra were generated using laser intensity 200, sensitivity 10, and mass focus between 10–160 kDa, to identify binding partners. The spectra were normalized to the 66 kDa peak representing albumin and set to the same scale.

Protein purification and identification

Anti-HSL IgG was conjugated to AminoLink Plus Coupling Resin (Pierce Biotechnology Inc, Rockford, IL, USA) and 250 μl of packed, anti-HSL IgG-conjugated beads were incubated with freshly prepared adipose cell lysates (3–4 mg/ml) overnight at 4°C. The beads were washed twice with phosphate-buffered saline containing 0.1% Triton X-100, and once with Tris-HCl buffer (pH 9.0) containing 1 M urea, 2% CHAPS, and 0.5 M NaCl. Captured proteins were then eluted with 50% acetonitrile/0.5% trifluoroacetic acid. The eluted proteins were run on SDS-PAGE under nonreducing conditions and stained with coumassie. Specific gel bands

were excised, destained, and dried followed by rehydration and digestion with trypsin at 37° C overnight. Aliquots (2 μl) of the tryptic digests were spotted onto NP20 ProteinChip Arrays (Ciphergen, Biosystems, Fremont, CA, USA). After addition of 20% a-cyano-4-hydroxycinnamic acid, peptide fragment masses were analyzed using the ProteinChip Biology System II and Ciphergen software. Peptide mapping was then analyzed using the ProFound database [31]. For confirmation and additional identification, tryptic digests were analyzed using Applied Biosystems QSTAR® Hybrid LCMSMS System with SELDI ProteinChip® Technology (Ciphergen Biosystems). Initial tryptic peptide maps were generated in single MS mode. A unique tryptic peptide of 1444 kDa was then analyzed for peptide fragmentation by MS/MS. Peptide sequencing was analyzed using Mascot [32].

Statistical analysis

Results are expressed as the mean±SE. Statistical significance was tested using ANOVA with Bonferroni as post test with InStat (version 3.0, GraphPad Software, San Diego, CA, USA) software for Macintosh.

Results

Identification of HSL-Interacting Protein Partners

To identify cellular proteins that might interact with HSL and, in this manner, participate in regulating the function of HSL in mediating lipolysis, recombinant, baculovirus-produced mouse HSL was used as bait and was immobilized to the surface of ProteinChip arrays from Ciphergen. The immobilized HSL protein chips were incubated with cell lysates prepared from adipose cells isolated from normal mice. After washing and incubation with an energy absorbing matrix, the proteins bound to the chip were analyzed by SELDI-TOF-MS. Figure 1 (upper panel) displays the results of this analysis and demonstrates that a number of adipose proteins between 10–125,000 Daltons appear to bind to the immobilized HSL, with clusters of proteins of 14.7 to 18.9 kDa, 25.8–26.8 kDa, 36.1 kDa, 44.3–49.1 kDa, and one at 53.7 kDa. As a control for the specificity of the binding of these adipose proteins to the protein chips, a parallel experiment was conducted with BSA immobilized to the protein chip in place of HSL. Figure 1 (lower panel) displays the results of the interaction of adipose cell lysates with immobilized BSA and shows only background signals, thus supporting the specificity of the interactions observed with immobilized HSL.

Identification of Hormonally Responsive HSL-Interacting Protein Partners

Since lipolysis and HSL translocation to the lipid droplet occur upon PKA stimulation, whereas anti-lipolysis occurs with insulin treatment, we sought to identify proteins whose interactions with HSL are hormonally dependent. Thus, we compared the pattern of the proteins that were prepared from isolated adipose cells that had been incubated for 30 min with either buffer alone (Control, C), isoproterenol (Iso) or isoproterenol plus insulin (Iso+Ins) for their ability to bind to immobilized, recombinant HSL. Each of the cell incubations was carried out in triplicate and is shown in Figure 2, where only proteins in the 40–60,000 Dalton range are emphasized. There was evidence for interaction of proteins prepared from control cells; however, lysates prepared from isoproterenol-treated cells showed a marked increase in the binding of several proteins in the 40–55,000 Dalton range, particularly one at 53.7 kDa. Interestingly, the pattern of the proteins bound to the immobilized HSL returned to baseline in the lysates prepared from cells treated with both isoproterenol and insulin. Thus, the results from these experiments appear to suggest that there are several proteins, particularly one with a mass of 53.7 kDa, that specifically interact with HSL under conditions of activation of PKA and that their ability to interact with HSL appears to be reversed by insulin treatment.

Identification of Hormonally Responsive HSL-Interacting Protein Partners By Immunocapture

Since the above experiments were conducted with immobilized recombinant HSL, using an experimental design that constitutes a “pull-down” experiment, independent evidence for the interaction of adipose proteins with endogenous HSL was conducted using protein chips with immobilized anti-HSL IgG to capture the HSL-protein complexes. As shown in Figure 3, where proteins in the 20–60,000 Dalton range are emphasized, a very similar pattern was observed, with several proteins of 20–60 kDa, particularly one with a mass of 53.7 kDa, appearing in lysates from cells treated with isoproterenol and disappearing in lysates from cells treated with both isoproterenol and insulin. These results provide additional evidence that several proteins, particularly one with a mass of 53.7 kDa, specifically interact with HSL under conditions of activation of PKA and that their ability to interact with HSL is reversed by insulin treatment.

Purification and Identification of the 53.7 kDa HSL-Interacting Partner

To achieve the identification of the 53.7 kDa protein that interacts with HSL, anti-HSL IgG was conjugated to agarose beads, and the anti-HSL IgG-conjugated beads were incubated with freshly prepared lysates from adipose cells that had been incubated with isoproterenol. After washing, the beads were eluted, and the captured proteins eluting off the beads were run on SDS-PAGE and stained with coumassie (Figure 4A). A protein of ~53 kDa was prominently observed in the initial elution, while smaller amounts of proteins of 95, 51 and 44 kDa were seen in subsequent elutions. The 53 kDa protein was excised from the gel and treated with trypsin. The trypsin digests were then spotted on ProteinChip arrays and analyzed by SELDI-TOF-MS (Figure 4B). Using this peptide map, the ProFound protein search engine [31] was employed for protein identification. The results revealed a complete identity covering 21% of vimentin, an intermediate filament known to form a scaffold around lipid droplets [33]. The 44 kDa protein was identified as glutamate ammonia ligase using similar methods, but further studies with it were not pursued.

As an additional means of confirming the identity of the 53.7 kDa protein, tryptic digests were analyzed using the Applied Biosystems QSTAR® Hybrid LCMSMS System with SELDI ProteinChip® Technology. Initial tryptic peptide maps were generated in single MS mode (Figure 4C), displaying an identical peptide map as in Figure 4B. A unique tryptic peptide of 1444 kDa was then analyzed for peptide fragmentation by MS/MS (Figure 4D). Peptide sequencing was analyzed using Mascot [32] and showed the peptide (SLYSSSPGGAYVTR) to be identical to vimentin.

Co-immunoprecipitation

To confirm the interaction of HSL with vimentin, cell lysates from adipose cells were immunoprecipitated with anti-HSL IgG and then immunoblotted with anti-vimentin antibody. As shown in Figure 5, vimentin was observed in cell lysates from control and isoproterenol-treated adipose cells, but not from insulin treated adipose cells, consistent with the interaction of vimentin with HSL being dependent on PKA phosphorylation. Conversely, attempts to immunoprecipitate with anti-vimentin IgG and then immunoblot with anti-HSL antibody were not successful. Immunoprecipitations using non-immune IgG showed no evidence for vimentin when immunoblotted with anti-vimentin antibodies (data not shown).

Effects of Vimentin on Lipolysis

To examine the involvement of vimentin in lipolysis, we compared the expression of some key components of lipolysis and droplet-associated proteins in white adipose tissue isolated from vimentin null and wild-type mice using real time RT-PCR to determine whether the loss of vimentin resulted in any alterations in the expression of genes involved in lipolysis and lipid

droplet formation. As shown in Figure 6A, mRNA expression for lipases such as ATGL, HSL, TGH and CGI-58 was normal or slightly increased when expressed relative to 36B4 mRNA in vimentin null compared to wild-type mice. Likewise, mRNA expression of droplet-associated proteins such as perilipin, ADRP, S3-12, and TIP47 was normal in vimentin null mice, though S3-12 tended to be slightly reduced. Immunoblot analysis of protein expression showed that, similar to mRNA levels, ATGL, HSL, CGI-58, perilipin, ADRP, and TIP47 were expressed similarly in white adipose tissue from vimentin null and wild-type mice (Figure 6B). Thus, the absence of vimentin does not seem to alter lipase or droplet-associated protein expression. In contrast, the ability to activate, i.e., phosphorylate, ERK, without a change in the total amount of ERK, was diminished in adipose cells isolated from vimentin null mice whether stimulated by incubation with isoproterenol, forskolin (PKA dependent and independent activation) or diacylglycerol (PKC dependent activation) (Figure 6C). Additionally, the absence of vimentin resulted in smaller adipose cell size (Figure 6D), with the entire population shifted toward smaller diameters. The mean cell diameter was 54.4±3.0 in vimentin null adipocytes versus 71.0±4.1 μm in wild-type ($p<0.02$). We next analyzed the dose-response of glycerol release of isolated adipocytes from vimentin null and wild-type mice to increasing concentrations of isoproterenol (Figure 7A). The maximal lipolytic response to isoproterenol was similar in adipocytes from vimentin null and wild-type mice, which is consistent with the basic components of lipolysis being intact in vimentin null mice. Interestingly, however, the dose response of vimentin null adipocytes to isoproterenol was significantly shifted to the right ($p<0.001$), consistent with less efficient lipolysis. To explore the effect of vimentin deficiency on the translocation of HSL to the lipid droplet, adipocytes isolated from vimentin null and wild-type mice were treated with isoproterenol and the amount of HSL detected to be associated with the fat cake was assessed at various times (Figure 7B). Under basal conditions, the amount of HSL associated with the fat cake was greater in adipocytes isolated from vimentin null mice ($p<0.05$). While the maximum association of HSL with the fat cake following isoproterenol stimulation was similar in adipocytes from vimentin null and wild-type mice, the rate of HSL translocation to the fat cake, i.e., the slope of the curve until maximum association with the fat cake was achieved, was slower ($p<0.05$) in vimentin null adipocytes.

Discussion

The mechanisms regulating lipolysis appear to be increasingly complex. The current mechanistic view proposes that the droplet-associated protein perilipin coats the lipid droplet and functions as a scaffold in the regulation of lipolysis [21, 34]. Under basal conditions, perilipin acts as a barrier to the hydrolysis of TAG within the droplet by preventing access to ATGL and HSL, the major lipases in adipose cells, through a poorly understood mechanism [15, 35]. Following activation of PKA by hormonal stimulation, perilipin and HSL are phosphorylated, which leads to dynamic changes in intracellular protein trafficking [21]. Phosphorylation of perilipin allows ATGL-mediated hydrolysis to proceed [36] and, concomitantly, the release of CGI-58 from its association with perilipin, where it is found under basal conditions [37, 38]. Phosphorylation of HSL leads to the movement of HSL from a cytosolic compartment, where it is primarily found in the basal state, to the lipid droplet [20]. The mechanisms mediating the translocation of HSL have not been fully elucidated, but it appears to involve perilipin [21, 39].

Previous work from our laboratory utilized a yeast 2-hybrid screen to try to identify interacting partners of HSL that might influence lipolysis. In that work we identified adipose fatty acid binding protein (FABP4) as an interacting partner of HSL and demonstrated that FABP4 was part of the lipolytic complex and functioned to sequester fatty acids, thereby preventing feedback inhibition of lipase activity [28, 30, 40, 41]. In the current experiments we used SELDI-TOF-MS to identify cellular proteins that might interact with HSL and, in this manner, participate in regulating the function of HSL in mediating lipolysis. Using recombinant HSL

as bait on protein chips, we identified clusters of proteins of 14.7 to 18.9 kDa, 25.8–26.8 kDa, 36.1 kDa, 44.3–49.1 kDa, and one at 53.7 kDa that interact with HSL, particularly when cell lysates were examined from adipose cells that had been treated with a β-agonist to activate PKA. Importantly, the ability to detect these interacting proteins was markedly diminished when the adipose cells had been treated with insulin. Moreover, a very similar pattern of proteins was identified when anti-HSL IgG was used as the bait instead of recombinant HSL.

Whether the phosphorylation of interacting partners, phosphorylation of HSL or phosphorylation of both partner and HSL is required for the observed interactions is not discernible from the current results and will require future studies to explore this. However, the fact that recombinant HSL was used as bait in some of the experiments and, as such, the bait would have not been available as substrate for PKA, suggests that phosphorylation of the interacting partners was important for mediating the interactions and capture observed. Nonetheless, this should be interpreted cautiously since HSL functions as a dimer [42]. Thus, even when recombinant HSL was used as bait, it is possible that endogenously phosphorylated HSL interacted with the observed partners and was captured on chips through an HSL-HSL interaction. Certainly, the translocation of HSL to the droplet has been shown to be dependent on PKA-mediated phosphorylation of HSL [20].

The identities of all the proteins captured on the protein chips using either HSL or anti-HSL IgG as bait have not been established, although the cluster of proteins of 14.7 kDa to 18.9 kDa is consistent with the size of FABPs, which we have previously demonstrated to interact with HSL [28, 40]. As the prominent protein observed on immunocapture, the identification of the 53.7 kDa protein was carried out by tryptic digestion and MS analysis, and determined to be vimentin. The interaction of HSL with vimentin, and its hormonal dependence, was confirmed by co-immunoprecipitation experiments, thus establishing a physical interaction between HSL and vimentin that appeared to be increased by stimulation of PKA and inhibited by insulin.

Vimentin is an intermediate filament that constitutes part of the network of the cytoskeleton [43]. It is expressed in mesenchymal cells, including adipocytes where it forms a cage or scaffold around lipid droplets [33], although it does not appear to surround all droplets. Several different reports of proteomic analyses of lipid droplets isolated from adipocytes have consistently identified vimentin as a droplet associated protein [6]. Vimentin has been shown to interact with several different proteins, including some with motor-like properties [44]. A number of different functions have been attributed to vimentin; however, vimentin null mice develop and reproduce normally and have no obvious phenotype [45]. Pre-adipocytes isolated and cultured *in vitro* from vimentin null mice were reported to have apparently normal accumulation and architecture of adipose lipid droplets [45]. Nonetheless, studies with vimentin null mice have revealed a role for vimentin in such functions as the localization and activity of the sodium-glucose cotransporter [46] and cytosolic PLA_2 [47]. Disruption of microtubules or microfilaments has been reported to have minimal effects on isoproterenol-stimulated glycerol release and no visible effects on the translocation of HSL determined by immunofluorescence light microscopy [48]. However, the agents which were previously used to disrupt microfilaments to study lipolysis and HSL translocation, e.g., nocodazole, cytochalasin, and cycloheximide [48], affect tubulin and actin, but have no effects on vimentin [49]. Using a proteomics approach, vimentin was recently identified as an interacting partner of agonist-stimulated β_3-adrenergic receptors and this interaction was shown to be important for activation of ERK and stimulation of lipolysis [50]. Previous studies have documented that ERK activation is responsible for ~30–40% of PKA stimulated lipolysis [2, 3] and the knockdown of vimentin by shRNA *in vitro* resulted in a loss of adrenergic receptor-mediated activation of ERK and a 40% reduction in lipolysis [50]. The current study employing primary adipose cells isolated from vimentin knockout mice confirmed that vimentin is required for agonist-stimulated activation of ERK. Additionally, the current studies documented a lower efficiency of lipolysis in adipose cells from vimentin

null mice, even though normal amounts of lipases and droplet-associated proteins, which are components of lipolysis, are expressed in these cells; however, maximal stimulated lipolysis was not altered. Moreover, greater amounts of HSL were observed to be associated with the fat cake under basal conditions in adipose cells from vimentin null mice; whereas the rate of HSL translocation was delayed in vimentin null adipocytes. Interestingly, vimentin null adipocytes were smaller than wild-type cells, suggesting that vimentin might participate in lipid droplet formation and/or homeostasis. Cell size has been reported to be decreased in mice with deletions of other intermediate filaments. For instance, hepatocytes are smaller in keratin 8 null mice [51] and keritonocytes are smaller in keratin 17 null mice [52]. Thus, although there are some apparent differences between *in vitro* knockdown studies and studies of cells from knockout animals, nonetheless, the results from the current studies provide evidence that vimentin might participate in lipolysis through direct interactions with HSL, in addition to its interaction with β-adrenergic receptors and the ERK signaling cascade.

Acknowledgments

The authors thank Jing Zhu and Sam Fu from Ciphergen for assistance. This work was supported in part by the Research Service of the Department of Veterans Affairs and National Institutes of Health Grant AG-028908 (to F.B.K.)

Abbreviations

PKA	cyclic AMP-dependent protein kinase
HSL	hormone-sensitive lipase
ATGL	adipose triglyceride lipase
TAG	triacylglycerol
DAG	diacylglycerol
CGI-58	comparative gene identification-58
SELDI	Surface Enhanced Laser Desorption/Ionization
TOF-MS	time-of-flight mass spectroscopy
TGH	triacylglycerol hydrolase
ADRP	adipose differentiation related protein

References

1. Duncan RE, Ahmadian M, Jaworski K, Sarkadi-Nagy E, Sul HS. Regulation of lipolysis in adipocytes. Annu Rev Nutr 2007;27:79–101. [PubMed: 17313320]
2. Greenberg AS, Shen W-J, Muliro K, Patel S, Souza SC, Roth RA, Kraemer FB. Stimulation of lipolysis and hormone-sensitive lipase via the extracellular signal-regulated kinase pathway. J Biol Chem 2001;276(48):45456–45461. [PubMed: 11581251]
3. Robidoux J, Kumar N, Daniel KW, Moukdar F, Cyr M, Medvedev AV, Collins S. Maximal beta3-adrenergic regulation of lipolysis involves Src and epidermal growth factor receptor-dependent ERK1/2 activation. J Biol Chem 2006;281(49):37794–802. [PubMed: 17032647]
4. Kraemer FB, Shen W-J. Hormone-sensitive lipase: control of intracellular tri-(di-) acylglycerol and cholesteryl ester hydrolysis. J Lipid Res 2002;43(10):1585–1594. [PubMed: 12364542]
5. Greenberg AS, Egan JJ, Wek SA, Garty NB, Blanchette-Mackie EJ, Londos C. Perilipin, a major hormonally regulated adipocyte-specific phosphoprotein associated with the periphery of lipid storage droplets. J Biol Chem 1991;266(17):11341–11346. [PubMed: 2040638]
6. Brasaemle DL, Dolios G, Shapiro L, Wang R. Proteomic analysis of proteins associated with lipid droplets of basal and lipolytically-stimulated 3T3-L1 adipocytes. J Biol Chem 2004;279:46835–46842. [PubMed: 15337753]

7. Liu P, Ying Y, Zhao Y, Mundy DI, Zhu M, Anderson RGW. Chinese hamster ovary K2 cell lipid droplets appear to be metabolic organelles involved in membrane traffic. J Biol Chem 2004;279(5): 3787–3792. [PubMed: 14597625]
8. Osuga, J-i; Ishibashi, S.; Oka, T.; Yagyu, H.; Tozawa, R.; Fujimoto, A.; Shionoira, F.; Yahagi, N.; Kraemer, FB.; Tsutsumi, O.; Yamada, N. Targeted disruption of hormone-sensitive lipase results in male sterility and adipocyte hypertrophy, but not in obesity. Proc Natl Acad Sci USA 2000;97:787–792. [PubMed: 10639158]
9. Villena JA, Roy S, Sarkadi-Nagy E, Kim KH, Sul HS. Desnutrin, an adipocyte gene encoding a novel patatin domain-containing protein, is induced by fasting and glucocorticoids: ectopic expression of desnutrin increases triglyceride hydrolysis. J Biol Chem 2004;279(45):47066–47075. [PubMed: 15337759]
10. Jenkins CM, Mancuso DJ, Yan W, Sims HF, Gibson B, Gross RW. Identification, cloning, expression, and purification of three novel human calcium-independent phospholipase A2 family members possessing triacylglycerol lipase and acylglycerol transacylase activities. J Biol Chem 2004;279:48968–48975. [PubMed: 15364929]
11. Wilson PA, Gardner SD, Lambie NM, Commans SA, Crowther DJ. Characterization of the human patatin-like phospholipase family. J Lipid Res 2006;47(9):1940–9. [PubMed: 16799181]
12. Zimmermann R, Strauss JG, Haemmerle G, Schoiswohl G, Birner-Gruenberger R, Riederer M, Lass A, Neuberger G, Eisenhaber F, Hermetter A, Zechner R. Fat mobilization in adipose tissue is promoted by adipose triglyceride lipase. Science 2004;306(5700):1383–1386. [PubMed: 15550674]
13. Haemmerle G, Lass A, Zimmermann R, Gorkiewicz G, Meyer C, Rozman J, Heldmaier G, Maier R, Theussl C, Eder S, Kratky D, Wagner EF, Klingenspor M, Hoefler G, Zechner R. Defective lipolysis and altered energy metabolism in mice lacking adipose triglyceride lipase. Science 2006;312(5774): 734–7. [PubMed: 16675698]
14. Kershaw EE, Hamm JK, Verhagen LA, Peroni O, Katic M, Flier JS. Adipose triglyceride lipase: function, regulation by insulin, and comparison with adiponutrin. Diabetes 2006;55(1):148–57. [PubMed: 16380488]
15. Miyoshi H, Souza SC, Zhang HH, Strissel KJ, Christoffolete MA, Kovsan J, Rudich A, Kraemer FB, Bianco AC, Obin MS, Greenberg AS. Perilipin promotes hormone-sensitive lipase-mediated adipocyte lipolysis via phosphorylation-dependent and -independent mechanisms. J Biol Chem 2006;281(23):15837–44. [PubMed: 16595669]
16. Lass A, Zimmermann R, Haemmerle G, Riederer M, Schoiswohl G, Schweiger M, Kienesberger P, Strauss JG, Gorkiewicz G, Zechner R. Adipose triglyceride lipase-mediated lipolysis of cellular fat stores is activated by CGI-58 and defective in Chanarin-Dorfman Syndrome. Cell Metab 2006;3(5): 309–19. [PubMed: 16679289]
17. Schweiger M, Schreiber R, Haemmerle G, Lass A, Fledelius C, Jacobsen P, Tornqvist H, Zechner R, Zimmermann R. Adipose triglyceride lipase and hormone-sensitive lipase are the major enzymes in adipose tissue triacylglycerol catabolism. J Biol Chem 2006;281(52):40236–41. [PubMed: 17074755]
18. Egan JJ, Greenberg AS, Chang MK, Wek SA, Moos MC Jr, Londos C. Mechanism of hormone-stimulated lipolysis in adipocytes: translocation of hormone-sensitive lipase to the lipid storage droplet. Proc Natl Acad Sci USA 1992;89:8537–8541. [PubMed: 1528859]
19. Clifford GM, Londos C, Kraemer FB, Vernon RG, Yeaman SJ. Translocation of hormone-sensitive lipase and perilipin upon lipolytic stimulation of rat adipocytes. J Biol Chem 2000;275(7):5011–5015. [PubMed: 10671541]
20. Su CL, Sztalryd C, Contreras JA, Holm C, Kimmel AR, Londos C. Mutational analysis of the hormone-sensitive lipase translocation reaction in adipocytes. J Biol Chem 2003;278:43615–43619. [PubMed: 12832420]
21. Granneman JG, Moore HP, Granneman RL, Greenberg AS, Obin MS, Zhu Z. Analysis of lipolytic protein trafficking and interactions in adipocytes. J Biol Chem 2007;282(8):5726–35. [PubMed: 17189257]
22. Sztalryd C, Xu G, Dorward H, Tansey JT, Contreras JA, Kimmel AR, Londos C. Perilipin A is essential for the translocation of hormone-sensitive lipase during lipolytic activation. J Cell Biol 2003;161(6):1093–1103. [PubMed: 12810697]

23. Wang J, Shen WJ, Patel S, Harada K, Kraemer FB. Mutational analysis of the “regulatory module” of hormone-sensitive lipase. Biochemistry 2005;44(6):1953–9. [PubMed: 15697220]
24. Eliasson C, Sahlgren C, Berthold CH, Stakeberg J, Celis JE, Betsholtz C, Eriksson JE, Pekny M. Intermediate filament protein partnership in astrocytes. J Biol Chem 1999;274(34):23996–4006. [PubMed: 10446168]
25. Sztalryd C, Hamilton J, Horwitz BA, Johnson P, Kraemer FB. Alterations of lipolysis and lipoprotein lipase in chronically nicotine-treated rats. Am J Physiol 1996;270:E215–E223. [PubMed: 8779941]
26. Shen WJ, Patel S, Yu Z, Jue D, Kraemer FB. Effects of rosiglitazone and high fat diet on lipase/esterase expression in adipose tissue. Biochim Biophys Acta 2007;1771(2):177–84. [PubMed: 17215164]
27. Sjostrom L, Bjorntorp P, Vrana J. Microscopic fat cell size measurements on frozen-cut adipose tissue in comparison with automatic determinations of osmium-fixed fat cells. J Lipid Res 1971;12(5):521–30. [PubMed: 5098392]
28. Shen W-J, Sridhar K, Bernlohr DA, Kraemer FB. Interaction of rat hormone-sensitive lipase with adipocyte lipid-binding protein. Proc Natl Acad Sci USA 1999;96(10):5528–5532. [PubMed: 10318917]
29. Harada K, Shen WJ, Patel S, Natu V, Wang J, Osuga J, Ishibashi S, Kraemer F. Resistance to high fat diet-induced obesity associated with altered expression of adipose specific genes in hormone-sensitive lipase deficient mice. Am J Physiol Endocrinol Metab 2003;285:E1182. [PubMed: 12954598]
30. Shen W-J, Liang Y, Hong R, Patel S, Natu V, Sridhar K, Jenkins A, Bernlohr DA, Kraemer FB. Characterization of the functional interaction of adipocyte lipid-binding protein with hormone-sensitive lipase. J Biol Chem 2001;276(52):49443–49448. [PubMed: 11682468]
31. Zhang W, Chait BT. ProFound: an expert system for protein identification using mass spectrometric peptide mapping information. Anal Chem 2000;72(11):2482–9. [PubMed: 10857624]
32. Perkins DN, Pappin DJ, Creasy DM, Cottrell JS. Probability-based protein identification by searching sequence databases using mass spectrometry data. Electrophoresis 1999;20(18):3551–67. [PubMed: 10612281]
33. Franke WW, Hergt M, Grund C. Rearrangement of the vimentin cytoskeleton during adipose conversion: formation of an intermediate filament cage around lipid globules. Cell 1987;49(1):131–41. [PubMed: 3548999]
34. Brasaemle DL. Thematic review series: Adipocyte Biology. The perilipin family of structural lipid droplet proteins: stabilization of lipid droplets and control of lipolysis. J Lipid Res 2007;48(12):2547–59. [PubMed: 17878492]
35. Souza SC, Muliro KV, Liscum L, Lien P, Yamamoto MT, Schaffer JE, Dallal GE, Wang X, Kraemer FB, Obin M, Greenberg AS. Modulation of hormone-sensitive lipase and protein kinase A-mediated lipolysis by perilipin A in an adenoviral reconstituted system. J Biol Chem 2002;277(10):8267–8272. [PubMed: 11751901]
36. Miyoshi H, Perfield JW 2nd, Souza SC, Shen WJ, Zhang HH, Stancheva ZS, Kraemer FB, Obin MS, Greenberg AS. Control of adipose triglyceride lipase action by serine 517 of perilipin A globally regulates protein kinase A-stimulated lipolysis in adipocytes. J Biol Chem 2007;282(2):996–1002. [PubMed: 17114792]
37. Subramanian V, Rothenberg A, Gomez C, Cohen AW, Garcia A, Bhattacharyya S, Shapiro L, Dolios G, Wang R, Lisanti MP, Brasaemle DL. Perilipin A mediates the reversible binding of CGI-58 to lipid droplets in 3T3-L1 adipocytes. J Biol Chem 2004;279(40):42062–71. [PubMed: 15292255]
38. Yamaguchi T, Omatsu N, Matsushita S, Osumi T. CGI-58 interacts with perilipin and is localized to lipid droplets. Possible involvement of CGI-58 mislocalization in Chanarin-Dorfman syndrome. J Biol Chem 2004;279(29):30490–7. [PubMed: 15136565]
39. Moore HP, Silver RB, Mottillo EP, Bernlohr DA, Granneman JG. Perilipin targets a novel pool of lipid droplets for lipolytic attack by hormone-sensitive lipase. J Biol Chem 2005;280(52):43109–20. [PubMed: 16243839]
40. Jenkins-Kruchten AE, Bennaars-Eiden A, Ross JR, Shen WJ, Kraemer FB, Bernlohr DA. Fatty acid-binding protein-hormone-sensitive lipase interaction: fatty acid dependence on binding. J Biol Chem 2003;278(48):47636–47643. [PubMed: 13129924]

41. Smith AJ, Sanders MA, Thompson BR, Londos C, Kraemer FB, Bernlohr DA. Physical association between the adipocyte fatty acid binding protein and hormone sensitive lipase: A fluorescence resonance energy transfer analysis. J Biol Chem 2004;279:52399–52405. [PubMed: 15456755]
42. Shen WJ, Patel S, Kraemer FB. Hormone-sensitive lipase functions as an oligomer. Biochemistry 2000;39:2392–2398. [PubMed: 10694408]
43. Fuchs E, Weber K. Intermediate filaments: structure, dynamics, function, and disease. Annu Rev Biochem 1994;63:345–82. [PubMed: 7979242]
44. Chou YH, Flitney FW, Chang L, Mendez M, Grin B, Goldman RD. The motility and dynamic properties of intermediate filaments and their constituent proteins. Exp Cell Res 2007;313(10):2236–43. [PubMed: 17498691]
45. Colucci-Guyon E, Portier MM, Dunia I, Paulin D, Pournin S, Babinet C. Mice lacking vimentin develop and reproduce without an obvious phenotype. Cell 1994;79(4):679–94. [PubMed: 7954832]
46. Runembert I, Queffeulou G, Federici P, Vrtovsnik F, Colucci-Guyon E, Babinet C, Briand P, Trugnan G, Friedlander G, Terzi F. Vimentin affects localization and activity of sodium-glucose cotransporter SGLT1 in membrane rafts. J Cell Sci 2002;115(Pt 4):713–24. [PubMed: 11865027]
47. Hirabayashi T, Murayama T, Shimizu T. Regulatory mechanism and physiological role of cytosolic phospholipase A2. Biol Pharm Bull 2004;27(8):1168–73. [PubMed: 15305015]
48. Brasaemle DL, Levin DM, Adler-Wailes DC, Londos C. The lipolytic stimulation of 3T3-L1 adipocytes promotes the translocation of hormone-sensitive lipase to the surfaces of lipid storage droplets. Biochim Biophys Acta 2000;1483(2):251–262. [PubMed: 10634941]
49. Collot M, Louvard D, Singer SJ. Lysosomes are associated with microtubules and not with intermediate filaments in cultured fibroblasts. Proc Natl Acad Sci USA 1984;81(3):788–92. [PubMed: 6366790]
50. Kumar N, Robidoux J, Daniel KW, Guzman G, Floering LM, Collins S. Requirement of vimentin filament assembly for beta3-adrenergic receptor activation of ERK MAP kinase and lipolysis. J Biol Chem 2007;282(12):9244–50. [PubMed: 17251187]
51. Galarneau L, Loranger A, Gilbert S, Marceau N. Keratins modulate hepatic cell adhesion, size and G1/S transition. Exp Cell Res 2007;313(1):179–94. [PubMed: 17112511]
52. Kim S, Wong P, Coulombe PA. A keratin cytoskeletal protein regulates protein synthesis and epithelial cell growth. Nature 2006;441(7091):362–5. [PubMed: 16710422]

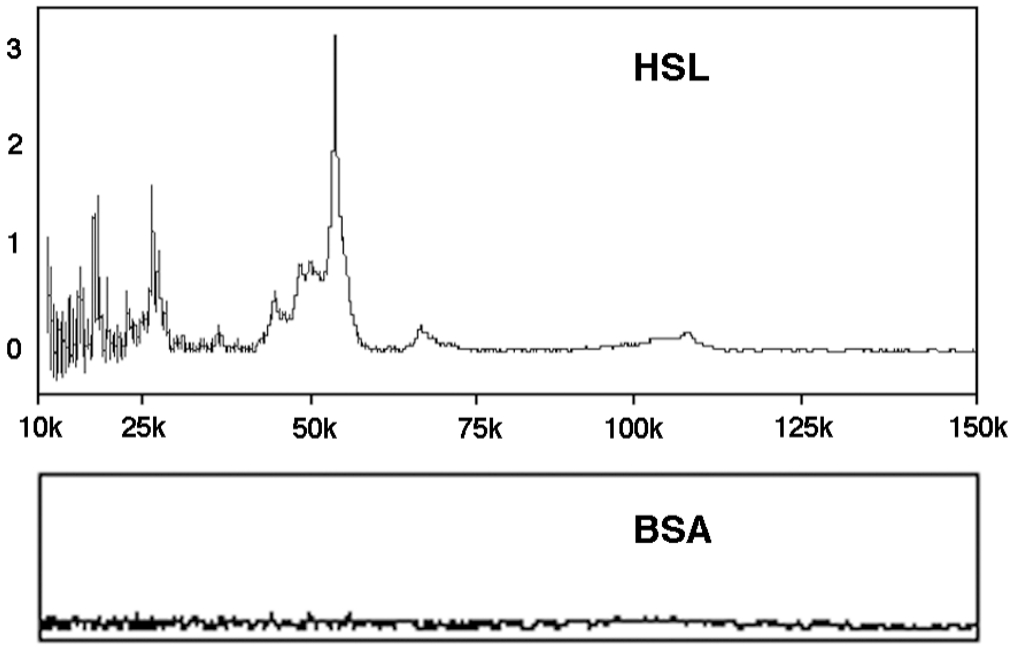

Figure 1.

SELDI-TOF-MS of adipose proteins binding to immobilized HSL (upper panel) or immobilized BSA (lower panel). Recombinant HSL (~0.5 μg) or BSA was immobilized on RS100 ProteinChip arrays. Unreacted amine groups were blocked with 0.5 M ethanolamine/phosphate-buffered saline for 1 h. The ProteinChips were washed three times for 5 min with phosphate-buffered saline containing 0.1% Triton X-100. Freshly prepared adipocyte lysates (2–4 mg/ml) were incubated with the arrays, then washed twice for 5 min with phosphate-buffered saline containing 0.1% Triton X-100 and once for 3 min with Tris-HCl buffer (pH 9.0) containing 1 M urea, 2% CHAPS, and 0.5 M NaCl. The ProteinChips were rinsed with 5 mM HEPES (pH 7.2) for 15 s and air-dried. A saturated solution of 3,5-dimethoxy-4-hydroxyinnamic acid (sinapinic acid) in 50% acetonitrile and 0.5% trifluoroacetic acid was applied to the ProteinChips and mass analysis was performed by SELDI-TOF-MS.

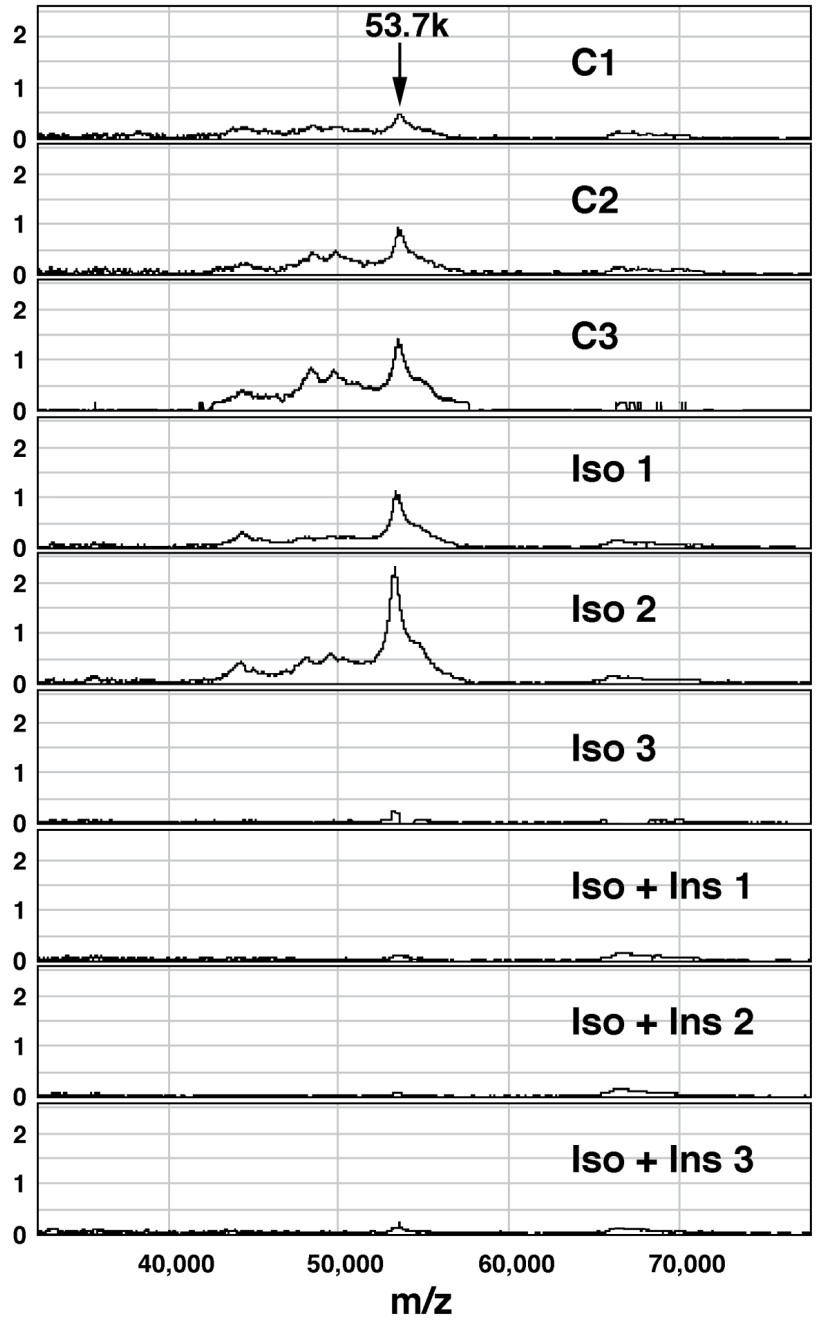

Figure 2.

SELDI-TOF-MS of proteins binding to immobilized HSL. Cell lysates were obtained from control (C), isoproterenol-treated (Iso, 1 μM) and isoproterenol (1 μM) plus insulin (100 μU/ml) - treated (Iso+Ins) primary wild-type mouse adipose cells. Each treatment was conducted with 3 independent incubations yielding 3 independent cell lysates. Data were obtained as described in Figure 1.

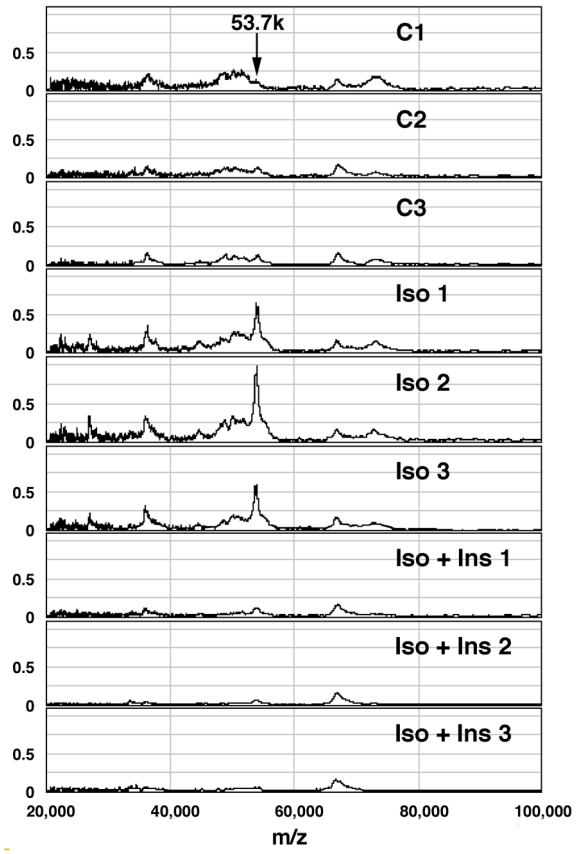

Figure 3.

SELDI-TOF-MS of proteins binding to immobilized anti-HSL IgG. Anti-HSL IgG (4μg) or BSA was immobilized on PS10 arrays and then treated as described in Figure 1. Cell lysates were obtained from control (C), isoproterenol-treated (Iso) and isoproterenol plus insulin-treated (Iso+Ins) primary wild-type mouse adipose cells. Each treatment was conducted with 3 independent incubations yielding 3 independent cell lysates.

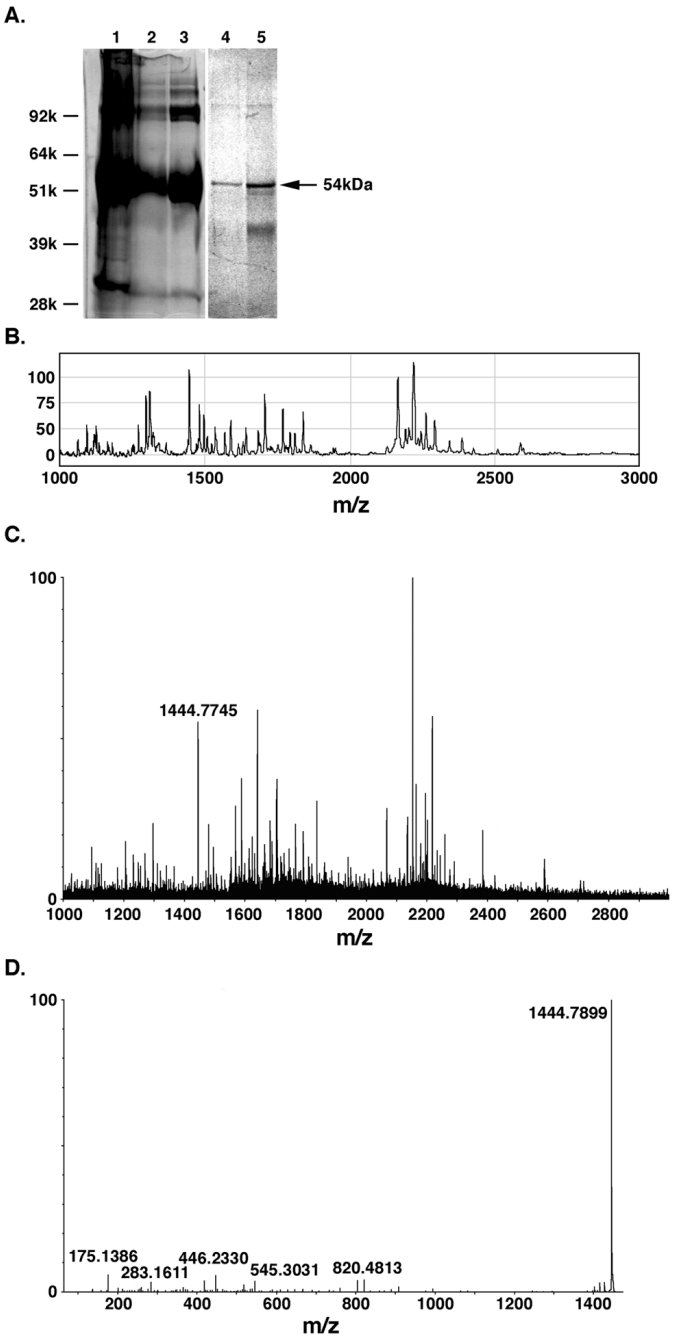

Figure 4.

Purification and Identification of the 53.7 kDa HSL-Interacting Partner. Panel A: Proteins captured on anti-HSL IgG-conjugated beads. Lane 1, wash; lane 2, flow through; lane 3 loading; lane 4, elution 1; lane 5, elution 2. Anti-HSL IgG was conjugated to AminoLink Plus Coupling Resin and 250 μl of packed, anti-HSL IgG-conjugated beads were incubated with freshly prepared adipose cell lysates (3–4 mg/ml) overnight at 4°C. The beads were washed twice with phosphate-buffered saline containing 0.1% Triton X-100, and once with Tris-HCl buffer (pH 9.0) containing 1 M urea, 2% CHAPS, and 0.5 M NaCl. Captured proteins were then eluted with 50% acetonitrile/0.5% trifluoroacetic acid. The eluted proteins were run on SDS-PAGE under nonreducing conditions and stained with coumassie. Panel B. SELDI-TOF-

MS of tryptic digests of the 53 kDa protein. Panel C: MS scan of the tryptic digests of the 53.7 kDa protein. Panel D: MS/MS analysis of peptide fragmentation of the 1444 Da peptide highlighted in Panel C.

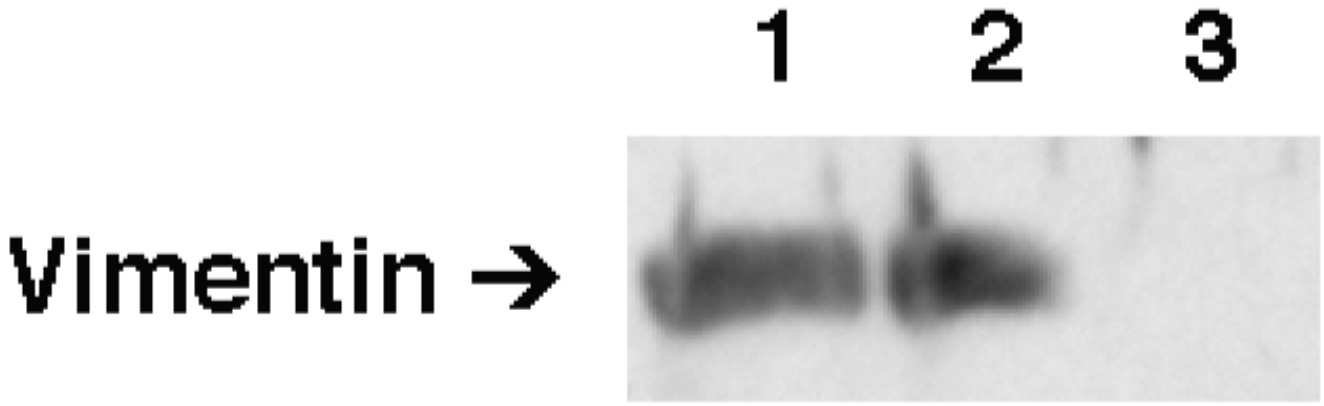

Figure 5.
Co-immunoprecipitation of vimentin and HSL. Cell lysates (250 μg) from adipose cells were immunoprecipitated with anti-HSL IgG and then immunoblotted with anti-vimentin antibody as described in the Materials and Methods. Lane 1, control adipose lysates; lane 2, lysates of adipose cells treated with isoproterenol (1 μM); lane 3, lysates of adipose cells treated with isoproterenol (1 μM) and insulin (100 μU/ml).

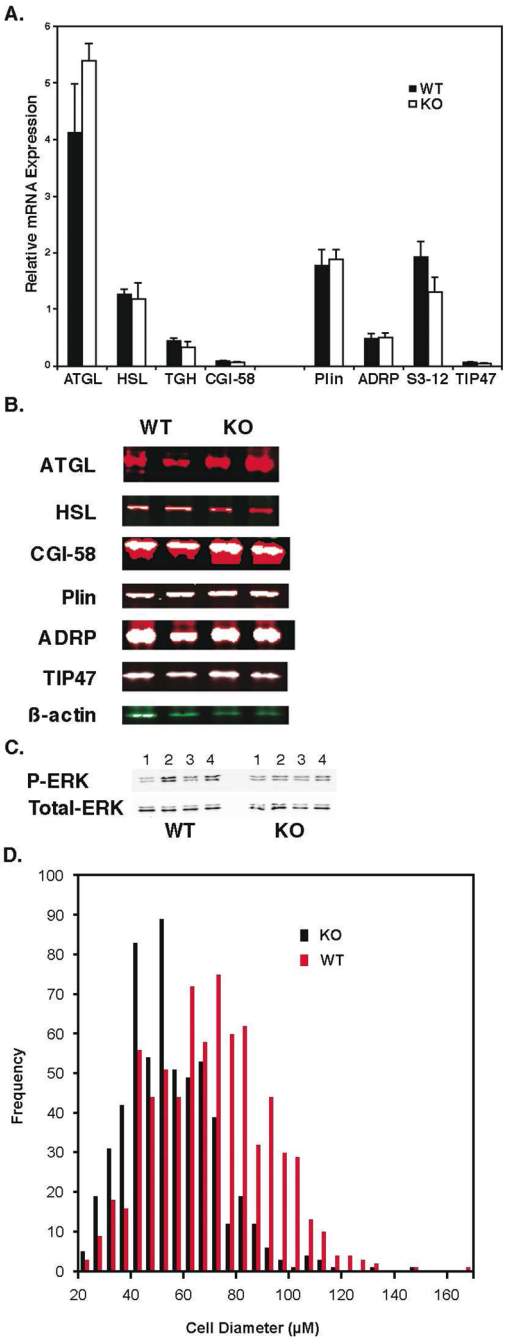

Figure 6.

Expression of lipases and droplet associated proteins in vimentin null (KO) and wild-type (WT) adipose tissue. Panel A: RT-PCR of mRNA expressed relative to 36B4. n=4 males in each group. Panel B: Immunoblot of total cell lysates. Cell lysates (20 µg) were resolved by 4–15% gradient SDS-PAGE gel, blotted onto nitrocellulose membranes, incubated with specific antibodies, and detected by infrared fluorescent imaging as described in the Materials and Methods. ATGL, adipose triglyceride lipase; HSL, hormone-sensitive lipase; TGH, triacylglycerol hydrolase; CGI-58, comparative gene identification-58; Plin, perilipin; ADRP, adipocyte differentiation related protein; TIP47, tail-interacting protein of 47 kDa. Panel C: Immunoblot of phosphorylated and total ERK in isolated adipocytes. Cell lysates (20 µg) were

resolved by 4–15% gradient SDS-PAGE gel, blotted onto nitrocellulose membranes, incubated with specific antibodies, and detected by chemiluminescence as described in the Materials and Methods. Lane 1, basal; lane 2, isoproterenol treated (0.5 μM); lane 3, forskolin treated (20 μM); lane 4, diacylglycerol treated (1 μM). P-ERK, phospho-extracellular signal-regulated kinase. Panel D. Adipose cell size in vimentin null (KO) and wild-type (WT) mice. n=6 WT and 5 KO mice.

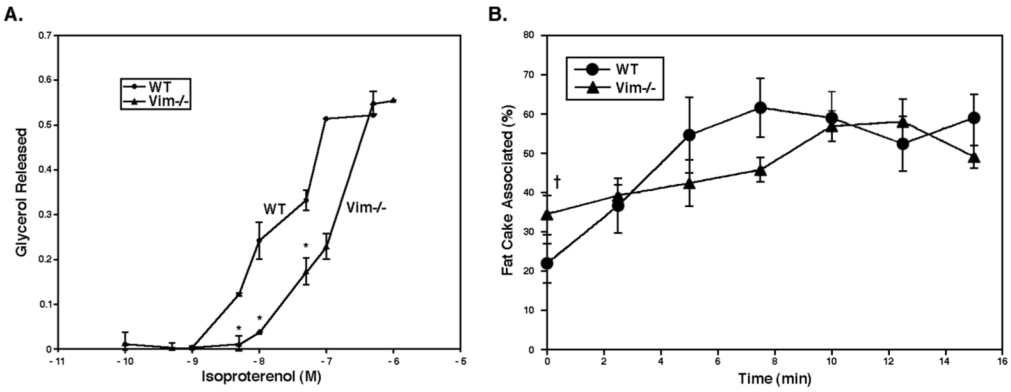

Figure 7.

Lipolysis in adipose cells from vimentin null mice. Panel A: Dose response of glycerol release to isoproterenol in adipose cells isolated from vimentin null (Vim−/−) and wild-type (WT) mice. Adipocytes isolated from 12–16 wks old vimentin null and wild-type littermates were incubated in the absence or presence of the indicated concentrations of isoproterenol in 120 mM NaCl, 4 mM KH_2PO_4, 1 mM $MgSO_4$, 1 mM $CaCl_2$, 10 mM $NaHCO_3$, 27 mM HEPES (pH 7.4) containing 3% BSA and 2.5 mM glucose for 60 min at 37°C in 95% air-5% CO_2. At the end of the incubation, an aliquot of infranatant was removed for measurement of glycerol concentration. *, $p<0.001$ Panel B: Time course of HSL association with the fat cake in adipose cells isolated from vimentin null (Vim−/−) and wild-type (WT) mice. Adipocytes isolated from vimentin null and wild-type littermates were incubated with isoproterenol (1 μM) as above for various times at 37°C in 95% air-5% CO_2. At the indicated times the cells were washed, homogenized, the fat cake and cytosol separated by centrifugation, and HSL detected by immunoblotting as described in the Materials and Methods. The results represent 4 independent experiments. †, $p<0.05$